COBEM 2021 Florianópolis - Brasil
26th ABCM International Congress of Mechanical Engineering
November 22-26, 2021. Florianópolis, SC, Brazil

COB-2021-0504
ON THE USE OF THE X-FEM METHOD FOR COMPUTATIONAL FRACTURE MECHANICS FOR MIXED MODE FRACTURE

José Airton Neiva Alves da Silva Brasil
Jorge Luiz de Almeida Ferreira
Universidade de Brasilía, Brasilía, Brazil
airton.bra@gmail.com
jorge@unb.br

Abstract. *In some structures the presence of a crack cannot be avoided. The severity of a crack in a structure can be described using the stress intensity factor, the calculation of these variables is particular for each case, and for each mode of fracture, taking into account the geometry, load case and crack size. In some structures, depending on the geometry, load case of crack position, exist a mixed mode fracture that take in account two or three fracture modes and each particular stress intensity for each mode has an effect on the severity of the presence of the crack, that can be described by an equivalent stress intensity factor, and in the crack propagation path, that can be described by angles that take into account the effects of each individual stress intensity factor. The Extended Finite Element Method (X-FEM) can be used in fracture mechanics for modeling the effects of cracks in a structure, in special in mixed mode fracture, where the crack propagation angles need calculation, that are harder in conventional finite element methods for fracture mechanics, because these methods need a better discretization and an updated mesh for each crack size advance. This work presents topics for the use of the X-FEM method for fracture mechanics, and uses the method to predict the crack propagation path, and their associated correlation factors, equivalent stress intensity factors and propagation angles, and the computational results are compared using experimental and analytical results obtained from the works of Ferreira (2017), Citarella et al. (2016), and Yates et al. (2007), that show, respectively, the change in the displacement field, that causes the mixed mode fracture, in the presence of the stress concentration, the presence of a multiaxial load case and the presence of multiple cracks. Showing that it is possible to obtain the computational results that are close to the experimental using the X-FEM method.*

Keywords: *Fracture Mechanics, Computational Fracture Mechanics, FEM, X-FEM.*

1. INTRODUCTION

The presence of a crack in a mechanical component can reduce its useful life causing a sudden catastrophic failure. In some components and structures these flaws are hard to, but the use of the fracture mechanics can be used to predict when the presence of a certain crack size is acceptable for a specific application.

For each geometry, loads and crack size, exists an equation that represents the stress intensity factor, this represents the severity of the problem. The computational fracture mechanics assists in the calculation of the stress intensity factor, but conventional finite elements methods for fracture mechanics are heavily dependent of the mesh, and for problems involving crack propagation the mesh update to each crack size are very time consuming, in especial in mixed mode fracture where the crack propagation path are harder to predict.

To solve these problems, Extended Finite Element Method (X-FEM) was developed to facilitate the modeling of discontinuities using an enriched space, that are less dependent of the mesh discretization.

2. X-FEM METHOD CONCEPTS

According to Kuna (2015), the Extended Finite Element Method (X-FEM) has the purpose of facilitate the modeling of discontinuities through the enrichment of the finite element unit partition. The idea is to enrich the classic finite element space using enrichment functions, which contain information from the solution. The enrichment functions add degrees of freedom in the discontinuity region to have a better precision in the solution, these functions should be chosen according to the analysis and the discontinuity.

According to Mohammadi (2008), the enrichment functions to the fracture mechanics have three main objectives: reproduce the singularity in the region of the crack tip; reproduce the effects of discontinuity in the displacement of adjacent elements; reproduce the independent displacement fields in two different sides of a surface.

2.1 Extrinsic enrichment

According to Malenk and Babuška (1996) the partition of unity applies the enrichment functions in the nodal shape functions, resulting in Eq. (1).

$$u(\boldsymbol{x}) = \sum_{i=1}^{M_{FEM}} N_i(\boldsymbol{x})\overline{\boldsymbol{u}}_i + \sum_{i=1}^{M_{XFEM}} N_i(\boldsymbol{x})\left(\sum_{j=1}^{M_{XFEM}} P_j(\boldsymbol{x})\overline{\boldsymbol{a}}_{\mathrm{ij}}\right) \tag{1}$$

where u is the displacement, $\overline{\boldsymbol{u}}$ is the nodal degrees of freedom vector, N is the shape function of classic finite element approach, P is the enriched shape function, $\overline{\boldsymbol{a}}$ is the enriched nodes degrees of freedom vector; and M_{FEM} is number of discretized nodes.

The extrinsic enrichment is based on partition of unity, that uses a global enrichment, increasing the computational effort, having the risk of not recognizing the discontinuity correctly, thus obtaining less accurate results. In contrast to the partition of unity, the extrinsic enrichment uses local enrichment, because discontinuities are usually local.

The enriched solutions can be written by Eq. (2).

$$u(\boldsymbol{x}) = \sum_{i=1}^{M_{FEM}} N_i(\boldsymbol{x})\overline{\boldsymbol{u}}_i + \sum_{j=1}^{M_{FEM}}\sum_{k=1}^{M_{XFEM}} \overline{N}_j(\boldsymbol{x})\psi_k(\boldsymbol{x})\overline{\boldsymbol{a}}_{\mathrm{kj}} \tag{2}$$

where M_{XFEM} is the number of enriched nodes, ψ is a enrichment function, and $\overline{N}$ is a shape function associated with the enriched node. The function $\overline{N}$ is not necessarily equal to N, but, accordingly Stazi *et al.* (2003), in a general way, can be used as equal as the conventional finite element method shape function, and it is recommended to use the linear form for high order elements, to assure a continuous calculation over a surface.

2.2 Heaviside function

Different discontinuity problems need different enrichments that considers the influence of it in the solution, the Heaviside function is used with problems where a discontinuity have different displacements fields in both sides (e.g., cracks).

The Heaviside enrichment function should give the information to represent a deformation field that includes all potential displacements field independently for both sides of the crack. The strain field also remain independent for both sides of the crack.

The application of the Heaviside function in a discontinuity field using the extrinsic enrichment can be seen in Eq. (3).

$$u(\boldsymbol{x}) = \sum_{i=1}^{M_{FEM}} N_i(\boldsymbol{x})\overline{\boldsymbol{u}}_i + \sum_{j=1}^{M_{FEM}}\sum_{k=1}^{M_{XFEM}} \overline{N}_j(\boldsymbol{x})H(\xi)\overline{\boldsymbol{a}}_{\mathrm{kj}} \tag{3}$$

where ξ is the local coordinate system, and H is the Heaviside enrichment function, that is defined by Bordas *et al.* (2007) as Eq. (4).

$$H(\xi) = \begin{cases} 0 & if\ \xi < -\beta \\ \dfrac{1}{2} + \dfrac{\xi}{2\beta} + \dfrac{1}{2\pi} sen\left(\dfrac{\pi\xi}{\beta}\right) & if\ -\beta < \xi < \beta \\ 1 & if\ \xi > \beta \end{cases} \tag{4}$$

where β is a small portion of element, smaller than the element size.

2.3 Asymptotic functions of the crack tip

The crack tip element can be partially cut by a discontinuity, in this situation the Heaviside function is not suitable to enrich the domain. In the regions in the vicinity of the crack tip it is used the asymptotic functions, that are based on exact functions for the displacement field. Considering the polar coordinates (r, θ) that have the origin in the crack tip, the enrichment asymptotic functions, as described by Fleming et al. (1998), can be seen in Eq. (5).

$$F(r,\theta) = \left\{\sqrt{r}sen\left(\frac{\theta}{2}\right), \sqrt{r}cos\left(\frac{\theta}{2}\right), \sqrt{r}sen\left(\frac{\theta}{2}\right)sen(\theta), \sqrt{r}sen\left(\frac{\theta}{2}\right)sen(\theta)\right\} \tag{5}$$

The first function in Eq. (5) is discontinued over the crack, representing the discontinuity in crack tip, and the other three functions are added to obtain precise results adding degrees of freedom in the nodes of the element containing the crack tip.

Combining the asymptotic enrichment function of the crack tip with the Heaviside function, the Eq. (6) is obtained.

$$u(\boldsymbol{x}) = \sum_{i=1}^{M_{FEM}} N_i(\boldsymbol{x})\bar{\boldsymbol{u}}_i + \sum_{k=1}^{M_{FEM}} \sum_{j=1}^{M_{XFEM}} \bar{N}_j(\boldsymbol{x})H(\xi)\bar{\boldsymbol{a}}_{\mathrm{kj}} + \sum_{l=1}^{M_{XFEM}} \sum_{m=1}^{Melement} \bar{N}_m(\boldsymbol{x})F(r,\theta)\mathbf{c_m} \tag{6}$$

where $\boldsymbol{c}$ is the degrees of freedom in the crack tip node element.

2.4 The level set method

Osher and Sethian (1988) developed the level set method to model the motion of interfaces, by this method is possible to represent an interface by the level set function and update this function with Hamilton-Jacobi equation knowing the speed of the interface in the normal direction.

Stolarska *et al.* (2001) coupled the level set function with X-FEM, where a crack can be described by two level sets:

- A normal level set, $\phi_N(\boldsymbol{x})$, that is the signed distance to the crack surface;
- A tangent level set, $\phi_T(\boldsymbol{x})$, that is the signed distance to the plane including the crack front and perpendicular to the crack surface.

The choose of the adequate enrichment function can be described as follow:

- If $\phi_{T\,min} < 0$ and $\phi_{N\,min}\phi_{N\,max} \leq 0$, then the crack cuts through the element and the nodes of the element are enriched with the Heaviside function;
- If $\phi_{T\,min}\phi_{T\,max} \leq 0$ and $\phi_{N\,min}\phi_{N\,max} \leq 0$, then the crack tip lies in the element and the nodes of the element are enriched with the crack tip asymptotic function.

2.5 The displacement correlation technique

With the X-FEM method is possible to obtain the displacement field for the problem, by using the displacement correlation technique is possible calculate the stress intensity factor by the nodal displacements in the crack front. Kuna (2015), presents equations to calculate the stress intensity factor, that can be seen in Eq. (7), (8) and (9).

$$K_I = \frac{E'}{8}\sqrt{\frac{2\pi}{L'}}\left\{2\mathrm{u}_2^B - u_2^C - 2u_2^E - u_2^F + u_2^D + \frac{1}{2}\xi_3(-4u_2^B + u_2^C + 4u_2^E - u_2^F) + \frac{1}{2}\xi_3^2(u_2^F + u_2^C - 2u_2^D)\right\} \tag{7}$$

$$K_{II} = \frac{E'}{8}\sqrt{\frac{2\pi}{L'}}\left\{2\mathrm{u}_1^B - u_1^C - 2u_1^E - u_1^F + u_1^D + \frac{1}{2}\xi_3(-4u_1^B + u_1^C + 4u_1^E - u_1^F) + \frac{1}{2}\xi_3^2(u_1^F + u_1^C - 2u_1^D)\right\} \tag{8}$$

$$K_{III} = \frac{E'}{8(1+\nu)}\sqrt{\frac{2\pi}{L'}}\left\{2\mathrm{u}_3^B - u_3^C - 2u_3^E - u_3^F + u_3^D + \frac{1}{2}\xi_3(-4u_3^B + u_3^C + 4u_3^E - u_3^F) + \frac{1}{2}\xi_3^2(u_3^F + u_3^C - 2u_3^D)\right\} \tag{9}$$

where the definitions of the subscripts A, B, C, D, E, F, H and the elemental length, L, can found in Figure 1.

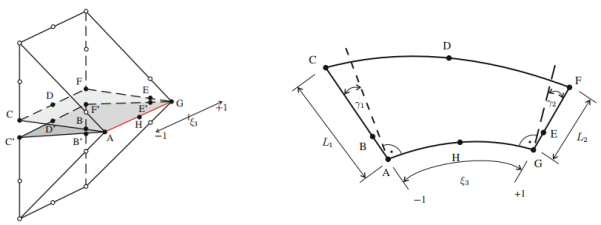

Figure 1. Quarter-point element used for displacement correlation technique. (Kuna, 2010)

3. MIXED-MODE OF FRACTURE

The mixed-mode loading conditions at crack can be observed in situations where, if due either the external loading, or component geometry or the orientation, the structure presents a non-symmetrical, singular stress field in the vicinity of the crack front. In that way, the crack front deforms in a opening and a planar or non-planar displacement and the crack front is defined by the stress factors K_I and/or K_{II} and K_{III}. The mixed-mode portions provoke the change of the crack growth direction, θ.

Richard, Fulland and Sander (2004) present a method to describe a mixed-mode stress intensity by a mode I equivalent stress intensity factor, this method can be described by Eq. (10).

$$K_{eq} = \frac{K_I}{2} + \frac{1}{2}\sqrt{K_I^2 + 4(1.155K_{II})^2 + 4K_{III}^2} = K_{Ic} \tag{10}$$

by this equation is possible calculate the equivalent stress intensity factor, K_{eq}, that causes the failure if it is equal to the critical mode I stress intensity factor, K_{Ic}.

Using the same method is possible observe the angles of deflection in crack propagation by Eq. (11) and (12).

$$\varphi = \pm\left[140°\left(\frac{|K_{II}|}{|K_I| + |K_{II}| + |K_{III}|}\right) - 70°\left(\frac{|K_{II}|}{|K_I| + |K_{II}| + |K_{III}|}\right)^2\right] \tag{11}$$

$$\psi = \pm\left[78°\left(\frac{|K_{III}|}{|K_I| + |K_{II}| + |K_{III}|}\right) - 33°\left(\frac{|K_{III}|}{|K_I| + |K_{II}| + |K_{III}|}\right)^2\right] \tag{12}$$

where φ is the angle of propagation in of the crack and ψ is the inclination of the crack.

4. METHODOLOGY

The theory of X-FEM method will be applied comparing three different components that have mixed-mode of fracture, the first one is a geometry with a presence of a hole in compact specimen, the computational results will be compared with the experimental results obtained in the work of Ferreira (2017); the second one is a cylindrical hollow specimen in the presence of combined tension-torsion loading, the computational results will be compared with the experimental results obtained in the work of Citarella *et al.* (2016); and the third one is a mixed-mode fracture caused by a presence of two cracks close to each other, the computational results will be compared with the experimental results of Yates *et al.* (2007).

The computational results that will be obtained are: crack propagation path, stress intensity factor represented by the correlation factor and non-dimensional length, and crack propagation angles.

The analyzed geometries can be seen in Figure 2.

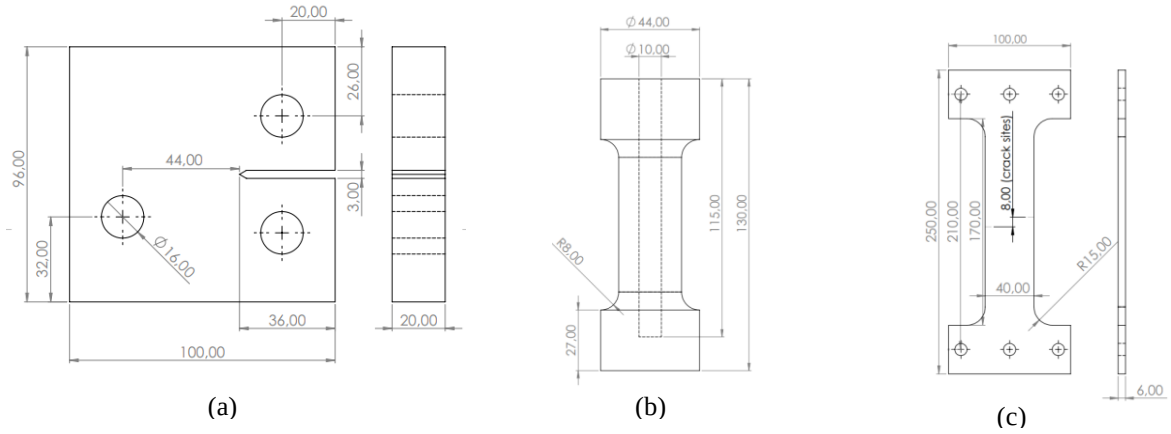

(a) (b) (c)

Figure 2. Geometries, mesh, and boundary conditions. (a) Geometry proposed by Ferreira (2017). (b) Geometry proposed by Citarella *et al.* (2016). (c) Geometry proposed by Yates *et al.* (2007).

and their respective mesh, boundary and loading conditions can been seen in Figure 3.

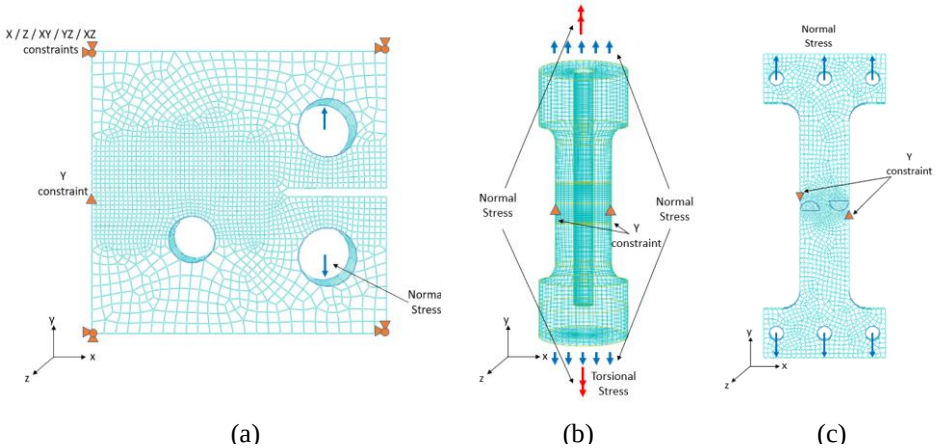

Figure 3. Mesh, and boundary conditions. (a) Geometry proposed by Ferreira (2017). (b) Geometry proposed by Citarella *et al.* (2016). (c) Geometry proposed by Yates *et al.* (2007).

The material used for the simulation was the aluminum alloy AA6082-T6, the material was characterized for a fracture analysis according to Ferreira (2017), and its proprieties can be seen in Table 1.

Table 1. Material proprieties for aluminum alloy AA6082-T6

Young modulus [MPa]	**Poisson ratio**	**Ultimate strength [MPa]**	**Yield strength [MPa]**	K_{th} **[MPa/$\sqrt{mm}$]**	K_c **[MPa/$\sqrt{mm}$]**
69000	0,33	310	260	136	1296

The simulation was performed using the commercial software ABAQUS, and the fracture properties, element separation and propagation characteristics was implemented using Abaqus Scripting Interface.

5. RESULTS

5.1 Crack path comparison

The crack propagation paths were obtained computationally and compared visually, with the experimental works used for comparison, and according to the position obtained.

The experimental results obtained by Ferreira (2017), Citerella *et al.* (2016) and Yates *et al.* (2007), and the computational results for crack path, are compared in Figures 4 to 6.

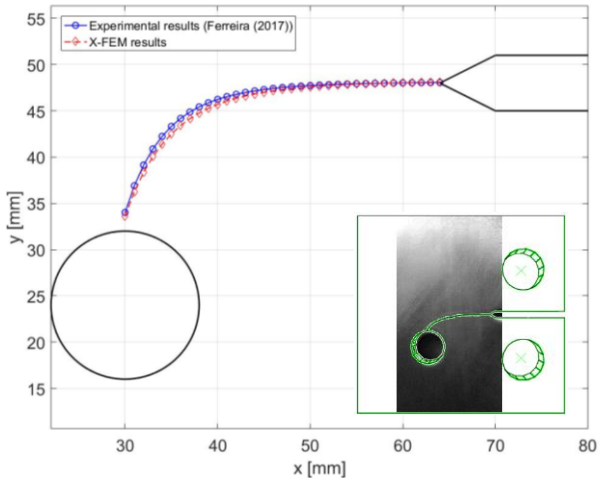

Figure 4. Comparison between the experimental and computational results and the experimental results obtained by Ferreira (2017)

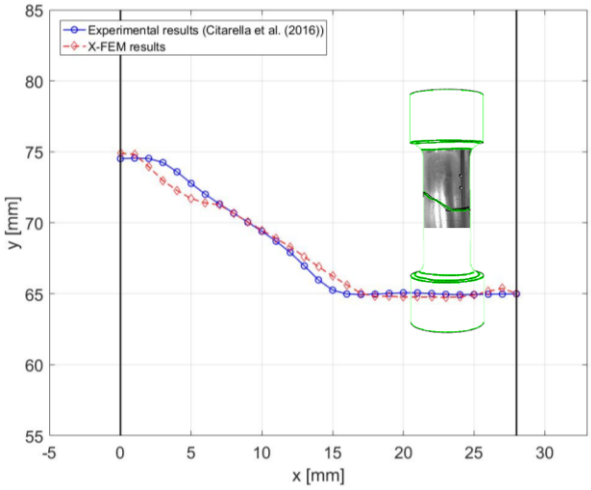

Figure 5. Comparison between the experimental and computational results and the experimental results obtained by Citarella *et al.* (2016)

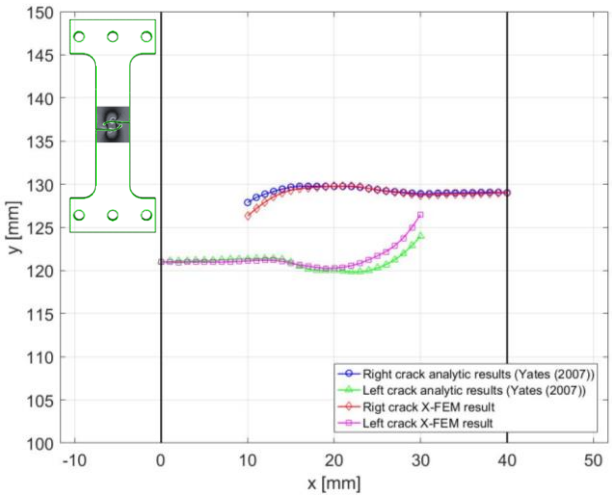

Figure 6. Comparison between the experimental and computational results and the experimental results obtained by Yates *et al.* (2007)

The relative errors between the experimental and computational is calculated for the y-axis positions for each x-axis position. The mean relative error obtained for the geometry proposed by Ferreira (2017) is 0,38 %. The mean relative error obtained for the geometry proposed by Citarella *et al.* (2007) is 0,73 %. The mean relative error obtained for the geometry proposed by Yates *et al.* (2016) is 0,54 %.

5.2 Stress intensity factor and Propagation angles

Using the paths obtained computationally the stress intensity factors was calculated and compared with the experimental works used for comparison. The results are show using the correlation factor, F, and a non-dimensional length, to avoid characterize the remote stress and the crack length. The stress intensity can be calculated by Eq. (13).

$$K = F\sigma\sqrt{\pi a} \tag{13}$$

The experimental results obtained by Ferreira (2017) and the computational results can be seen in Figure 5. The non-dimensional crack length is calculated by a/L, where L is the distance between the tip of the notch to the center of the hole, and a is measured in the surface, where $a_{position} = \sqrt{x_{position}^2 + y_{position}^2}$. The propagation angles and equivalent stress intensity factor was calculated using a nominal normal stress of 50 MPa.

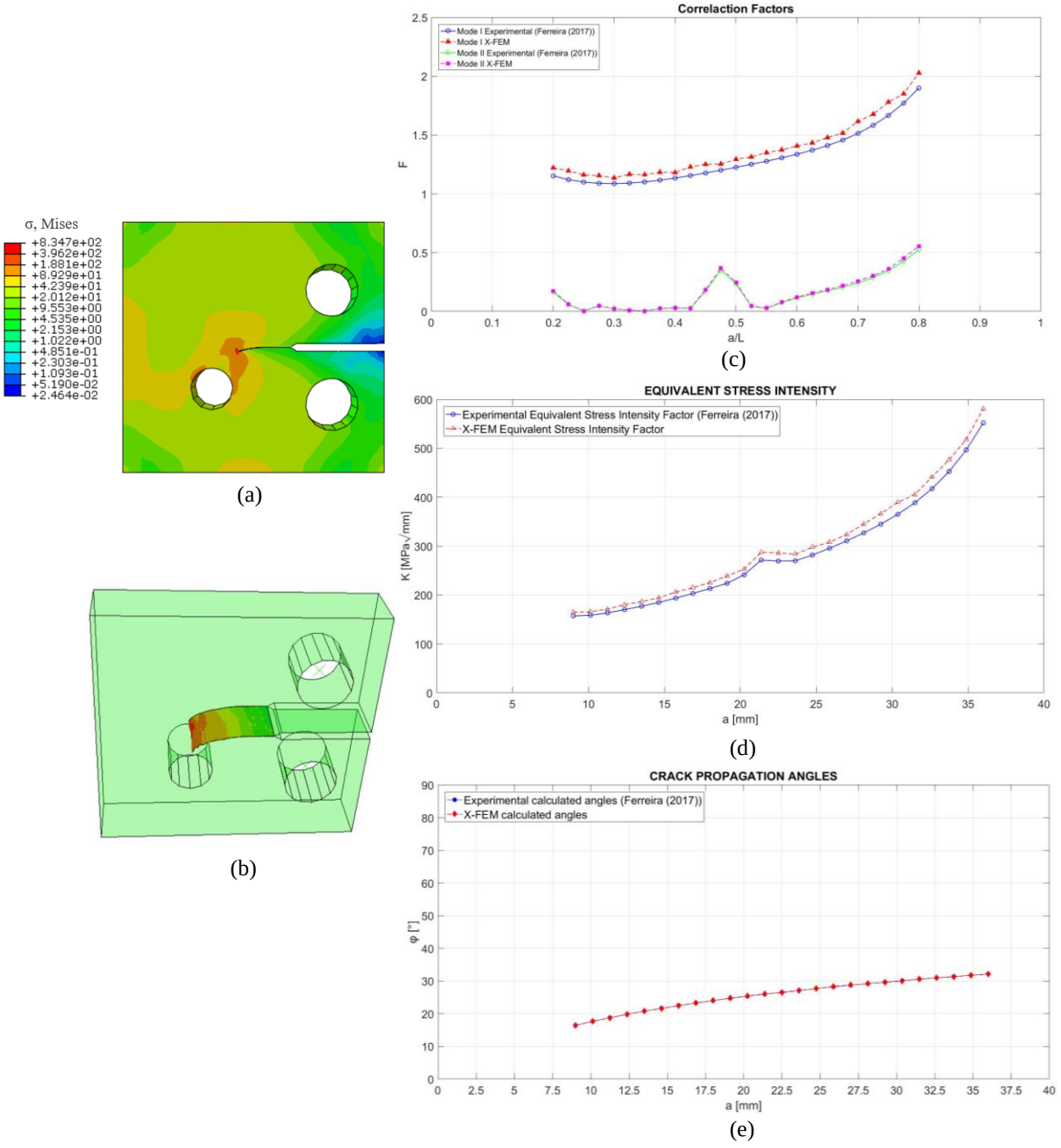

Figure 4. Comparison between the experimental, obtained by Ferreira (2017), and computational correlation factors and propagation angles. (a) Stress plot in a mixed mode fracture problem using X-FEM method. (b) Crack surface obtained computationally. (c) Correlation Factor for Mode I and II. (d) Equivalent Mode Stress Intensity Factor for a nominal normal stress equal to 50 MPa. (e) Propagation angles for a nominal normal stress equal to 50 MPa.

The Equivalent Mode Correlation factor presented a mean relative error of 5,47 % between the experimental and X-FEM results. And the calculated angles had a relative error of 0,28 %.

The experimental results obtained by Citarella *et al.* (2016) and the computational results, can been seen in Figure 6. The non-dimensional crack length is calculated by a/R, where a is the crack length, measured in the surface, and R is the external perimeter of the cylindrical specimen. The equivalent stress intensity factor for this specific problem was calculated using a nominal normal stress of 50 MPa and a nominal torsional stress of 92 MPa.

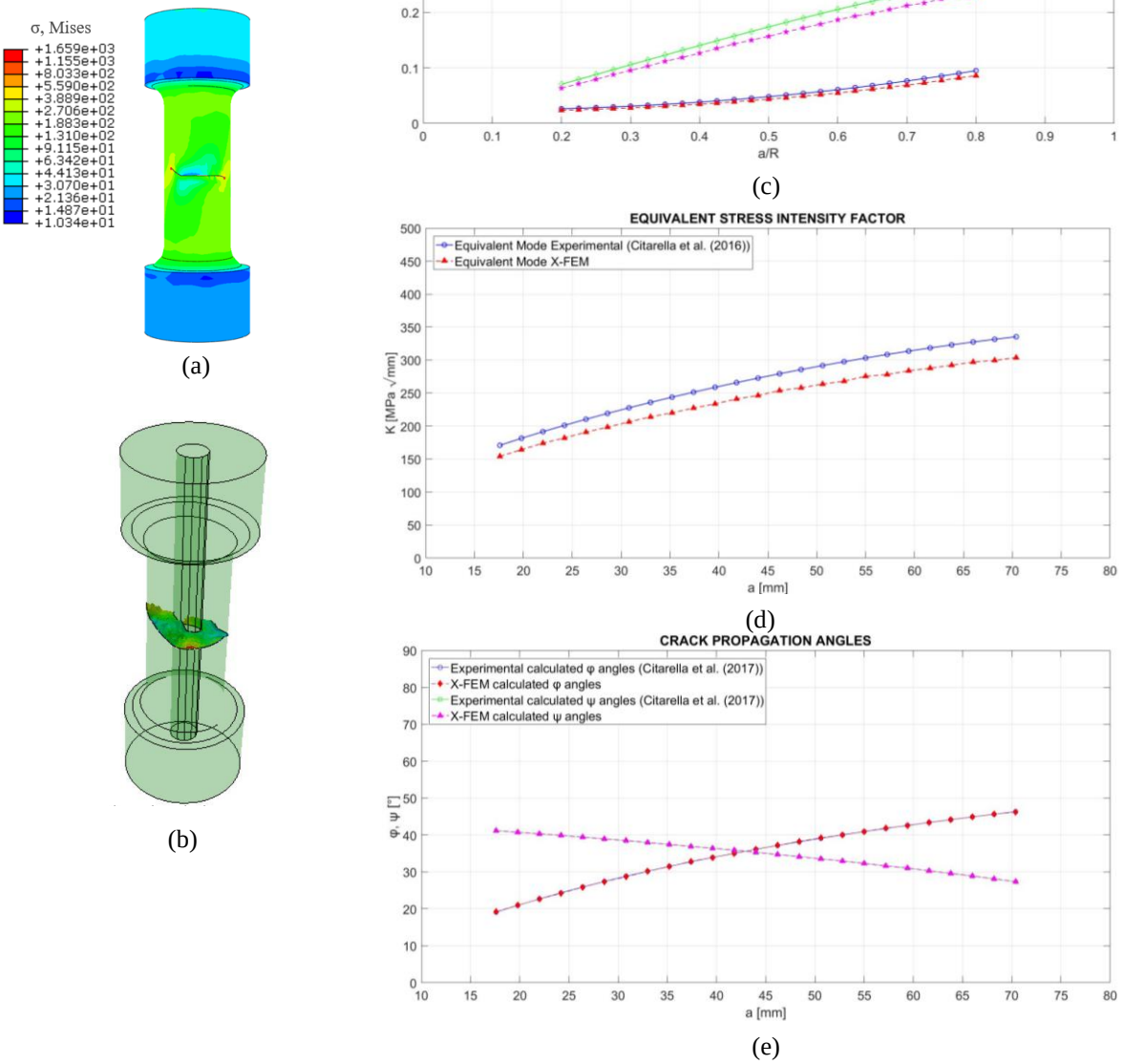

Figure 5. Comparison between the experimental, obtained by Citarella *et al.* (2016), and computational correlation factors and propagation angles. (a) Stress plot in a mixed mode fracture problem using X-FEM method. (b) Crack surface obtained computationally. (c) Correlation Factor for Mode I, II and III. (d) Equivalent Mode Stress Intensity Factor for this specific problem

The Equivalent Mode Correlation factor presented a mean relative error of 9,44 % between the experimental and X-FEM results. And the calculated φ angles had a relative error of 0,16 % and for the calculated ψ angles had a relative error of 0,74 %.

The experimental results obtained by Yates *et al.* (2007) and the computational results for correlation factors and the equivalent stress intensity, can been seen in Figure 6. The non-dimensional crack length is calculated by a/W, where W is equal to the length of the specimen. The equivalent stress intensity factor is for this specific problem using a nominal normal stress of 73 MPa.

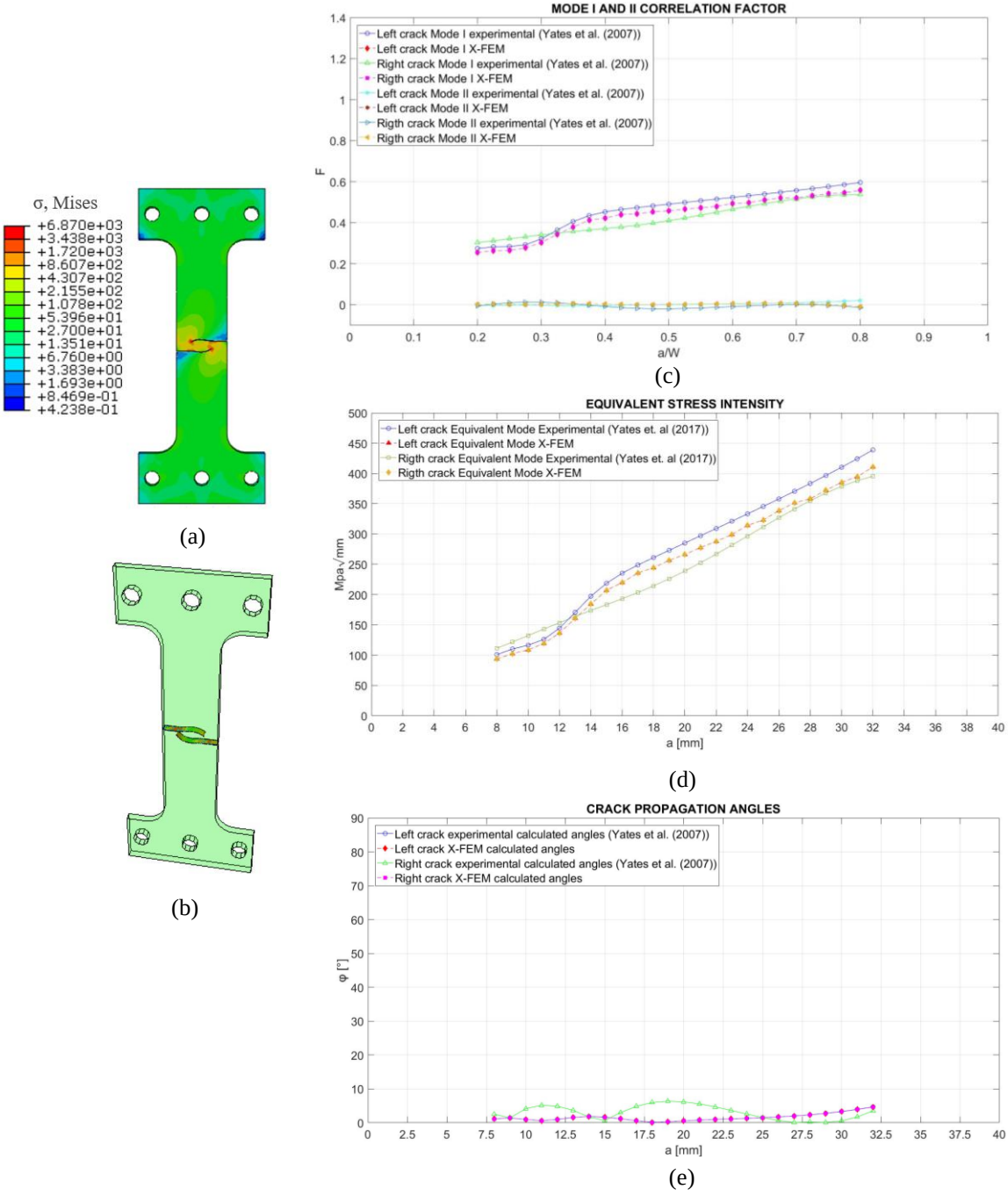

Figure 6. Comparison between the experimental, obtained by Yates *et al.* (2007), and computational correlation factors and propagation angles. (a) Stress plot in a mixed mode fracture problem using X-FEM method. (b) Crack surface obtained computationally. (c) Correlation Factor for Mode I, II and III. (d) Equivalent Mode Stress Intensity Factor for this specific problem

The Equivalent Mode Correlation factor presented a mean relative error of 5,92 % between the experimental and X-FEM results for the left crack and a mean relative error of 18,91 % between the experimental and X-FEM results for the right crack. And the calculated angles for the left crack had a relative error of 0,97 % and the calculated angles for the right crack had a relative error of 16,85 %. The computational results for both cracks are equal.

6. CONCLUSIONS

The analysis of mixed mode fracture using the X-FEM method presented consistent results if compared to the experimental results, except for the right crack of the Yates *et al.* (2007) geometry, where the experimental results presented a different results between the parallel cracks in the results of the correlation factors for Mode I, and

consequently for the calculated results of the equivalent stress intensity and propagation angles, but was expected that both crack presented same results, as presented in the X-FEM method analysis.

Some considerations could be made based on the analysis and results:

- The X-FEM could handle the mixed mode fracture and presented consistent results without the need of a great discretization of the mesh, where conventional methods need at least the spider-web configuration of the mesh in the crack tip, and could handle the crack propagation without the need of a mesh update;
- The crack propagation path and angles for crack propagation presented very similar results with the experimental (error < 1 %), although the calculations of the correlation factors and equivalent stress intensity between the experimental and the computational presented errors greater than 5 %, that is, the proportionality between the modes I, II and III, that controls the crack propagation path and angles, has remained almost the same;
- The experimental work of Yates *et al.* (2007), was made using thermoelastic stress analysis, and presented different results between the right crack and the left, although was expected the same, but in opposite direction of propagation, that could happen because the material and structure in experimental analysis not always responds as idealized, but a simulation, that was not programmed to analyze a particular response, will act as idealized.

7. ACKNOWLEDGEMENTS

My thanks to CNPq for funding this research, to the Universidade de Brasília, and the GFFM.

8. REFERENCES

Bordas, S., Nguyen, P. V., Dunant, C., Guidoum, A., Nguyen-Dang, H., 2007. “An extended finite element library”. *International Journal for Numerical Methods in Engineering*, Vol. 71, No. 6, pp.703–732.

Citarella, R., Sepe, R., Giannella, V., Ishtyryakov, I., 2016. “Multiaxial Fatigue Crack Propagation of an Edge Crack in a Cylindrical Specimen Undergoing Combined Tension-Torsion Loading”. *Procedia Structural Integrity*, Vol. 2, pp. 2706–2717.

Ferreira, M. A, 2017. *Mixed mode crack propagation: Numerical and Experimental Study.* Master’ degree dissertation. Faculdade de engenharia da Universidade do Porto, Porto, Portugal. 93 pp.

Fleming, M., Chu, Y. A., Moran, B., Belytschko, T., 1998. “Enriched Element-Free Galerkin Methods for Crack Tip Fields”. *International Journal for Numerical Methods in Engineering*, Vol; 40, No. 8, p. 1483–1504.

Fries, T. P., Belytschko, T., 2006. “The Intrinsic XFEM: A Method for Arbitrary Discontinuities Without Additional Unknowns”. *International Journal for Numerical Methods in Engineering*, Vol. 68, No. 13, p. 1358–1385.

Fries, R. G., Kearney, V. E., Engle R. M., 2010. “The Extended/Generalized Finite Element Method: An Overview of The Method and Its Applications”. *International Journal for Numerical Methods in Engineering*, Vol. 84, No. 3. pp. 253–304.

Kuna, M., 2015. *Finite Elements in Fracture Mechanics.* 1 ed. Springer. Freiberg, Germany. pp. 21–317.

Melenk, J. M., Babuška, I., 1996. “The Partition of Unity Finite Element Method: Basic Theory and Applications”. *Computer Methods in Applied Mechanics and Engineering*, Vol. 139, No. 15, p. 289–314.

Mohammadi, S., 2008, *Extended Finite Element Method*. Blackwell Publishing Ltd. Tehran, Iran. pp. 61–115.

Osher, S., Sethia, J. A., 1988, “Fronts propagating with curvature-dependent speed: Algorithms based on Hamilton-Jacobi formulations”. *Journal of Computational Physics,* Vol. 79, No. 1, pp. 12-49.

Richard, H. A., Fulland, M., Sander, M., 2004. “Theoretical crack path prediction”. *Fatigue & Fracture of Engineering Materials & Structures*, Vol. 28, No. 1-2, pp. 3–12.

Richard, H. A., Fulland, M., Sander, M., 2004. “Theoretical crack path prediction”. *Fatigue & Fracture of Engineering Materials & Structures*, Vol. 28, No. 2, pp. 3–12.

Storlaska, M., Chopp, D.L, Moes, N., Belyschko, T., 2001, “Modeling crack growth by level sets in the extended finite element method”. *International Journal for Numerical Methods in Engineering,* Vol. 51, pp. 943–960.

Yates, J. R., Zanganeh, M., Tomlinson, R. A., Brown, M. W., Garrido, F. A., 2007. “Crack paths under mixed mode” loading. *Engineering Fracture Mechanics,* Vol. 75, pp. 319–330.

Yazid, A., Abdelkader, N., Abdelmadjid, H., 2009. “A State-of-the-Art Review of the X-FEM for Computational Fracture Mechanics”. In: *Applied Mathematical Modelling*. Vol. 33, p. 4269–4282.

9. RESPONSIBILITY NOTICE

The authors are the only responsible for the printed material included in this paper.